Available online at www.sciencedirect.com
ScienceDirect
Scripta Materialia 64 (2011) 1043–1046
Scripta MATERIALIA
www.elsevier.com/locate/scriptamat

Energy barrier for homogeneous dislocation nucleation: Comparing atomistic and continuum models

Sylvie Aubry,[a] Keonwook Kang,[a] Seunghwa Ryu[b] and Wei Cai[a,*]

[a]*Department of Mechanical Engineering, Stanford University, CA 94305-4040, USA*
[b]*Department of Physics, Stanford University, Stanford, CA 94305, USA*

Received 2 December 2010; revised 14 February 2011; accepted 15 February 2011
Available online 23 February 2011

We compare the energy barriers predicted by continuum mechanics models for homogeneous dislocation nucleation in copper with explicit atomistic calculations. We find that a relatively simple continuum model can agree with full atomistic calculations if the dislocation Burgers vector is allowed to increase continuously during nucleation. The analysis identifies the significant effect of the applied shear stress on the generalized stacking fault energy and leads to a more physical definition of the ideal shear strength.

Keywords: Dislocation; Plastic deformation; Thermally activated processes; Atomistic simulations; Continuum models

Dislocation is one of the most important defects responsible for the plastic deformation of crystals. Dislocation nucleation is particularly important in small volumes where dislocations are either absent in the initial condition [1] or can easily leave the crystal [2]. According to the classical nucleation theory [3], the rate of dislocation nucleation is determined, to a large extent, by its energy barrier. Both atomistic simulations [4] and continuum models [5–11] have been used to predict the energy barrier for dislocation nucleation, but, surprisingly, their predictions have never been compared quantitatively against each other. The purpose of this letter is to construct such a bridge between atomistic and continuum models, and to gain a deeper understanding of the dislocation nucleation mechanism through this exercise.

The atomistic calculations of energy barriers are usually performed by the nudged-elastic band (NEB) [12] or the string method [13]. Two atomistic configurations, namely state $\mathcal{A}$ and state $\mathcal{B}$, are created corresponding to the states before and after the nucleation. The NEB (or string) method is then used to search for a (local) minimum energy path (MEP) connecting the two. The energy barrier is the maximum energy along the MEP in excess to state $\mathcal{A}$. The search for the MEP needs to be repeated for each stress of interest, and is rather time consuming. The accuracy of the predicted energy barrier also depends on the quality of interatomic potential in the atomistic model.

Various continuum models have also been developed for dislocation nucleation. The earliest model considers the energy variation of a circular dislocation loop with constant Burgers vector and changing loop radius [5], and is still used today [9]. The energy barrier predicted by this model is usually very high. It was later realized that the energy barrier can reduce significantly if the magnitude of the Burgers vector is allowed to change during nucleation [6,7,10]. More sophisticated continuum models have been developed, in which the Burgers vector is continuously distributed over the slip plane [6,8,11]. Given the spectrum of continuum models, it is of interest to know what level of complexity is necessary and sufficient to capture the behavior of explicit atomistic models.

In this letter, we show that a relatively simple two-variable continuum model, based on Burgers vector and loop radius, is able to match the atomistic results, provided that it takes the generalized stacking fault energy as an input and the dislocation core radius as a fitting parameter. In addition, the applied shear stress is found to significantly reduce the generalized stacking fault energy. This effect causes a further reduction of the dislocation nucleation energy barrier that is previously unnoticed and leads to a more physical definition of the ideal shear strength.

Our model is a perfect crystal of copper, with dimensions $8[1\,1\,\bar{2}] \times 6[1\,1\,1] \times 13[1\,\bar{1}\,0]$, described by the embedded-atom method (EAM) potential [14]. Periodic boundary conditions (PBC) are applied in all three directions. The simulation cell is subjected to a shear

* Corresponding author. E-mail: caiwei@stanford.edu

1359-6462/$ - see front matter © 2011 Acta Materialia Inc. Published by Elsevier Ltd. All rights reserved.
doi:10.1016/j.scriptamat.2011.02.023

strain γ_{xy}, with other strain components adjusted so that σ_{xy} is the only non-zero stress component. Figure 1a shows the shear stress–strain curve of the perfect crystal at zero temperature. At each stress (strain) condition, the crystal structure thus obtained is the state $\mathcal{A}$ for the MEP search.

We consider the homogeneous nucleation of a Shockley partial dislocation on the (1 1 1) plane with Burgers vector $\mathbf{b}_p = [1\,1\,\bar{2}]/6$ [15]. We focus on the partial dislocation because the nucleation of the leading partial is usually the rate limiting step of slip or twinning initiation [4]. The state $\mathcal{B}$ for the MEP search is the crystal containing a dislocation loop with Burgers vector $\mathbf{b}_p$ and radius $R = 25$ Å. The radius is chosen to be large enough so that the loop will spontaneously expand under the stress range in this work ($\sigma_{xy} > 2$ GPa). In order to reduce computation time, we intentionally make state $\mathcal{B}$ not a metastable state so that it is not too far away from the saddle configuration. To search for the MEP between our states $\mathcal{A}$ and $\mathcal{B}$, we modify the string method to add an additional constraint that the total length of the path remains constant during the relaxation. This prevents state $\mathcal{B}$ from falling into a metastable state [16] (in which the dislocation loop completely shears one crystallographic plane), so that the entire transition path can be well sampled using 20 replicas. The converged energy barrier as a function of applied shear stress is plotted in Figure 1b in filled circles. It will serve as the reference value for our continuum models.

In the following, we introduce three continuum models with increasing levels of complexity and compare their predictions with atomistic data shown in Figure 1b and c.

The simplest model starts with the energy of a circular dislocation loop with Burgers vector $\mathbf{b}_p$ and area A,

$$E(A;\sigma) = 2\pi R\,\frac{\mu b^2}{8\pi}\left[\frac{2-\nu}{1-\nu}\left(\ln\frac{8R}{a}-2\right)+\frac{1}{2}\right] + \gamma_{\mathrm{SF}}A - b\sigma A \tag{1}$$

where μ is shear modulus and ν is Poisson's ratio. $R = \sqrt{A/\pi}$ is the radius of the loop. $b = |\mathbf{b}_p|$ and the subscript $_{xy}$ is omitted in σ for brevity. a is the core cut-off radius [17]. The first term in Eq. (1) is the elastic energy. The second term is the stacking fault energy because a partial (instead of perfect) dislocation is nucleated. The last term represents the work done by the applied shear stress, which drives dislocation nucleation. The energy barrier for dislocation nucleation at a given stress σ is simply obtained from the maximum of Eq. (1), i.e. $E_{\mathrm{b}}^{\mathrm{I}}(\sigma) = \max_{A>0} E(A;\sigma)$ where the superscript $^{\mathrm{I}}$ indicates model I.

Most of the material parameters in Eq. (1) are determined from the EAM potential [14], e.g. $\gamma_{\mathrm{SF}} = 44.7\ \mathrm{mJ/m^2}$. The effective isotropic elastic constants, $\mu = 44.6$ GPa and $\nu = 0.41$ (see Supplementary materials), are determined from the cubic elastic constants of the EAM potential using the approach of Scattergood and Bacon [18]. Unfortunately, the core radius a is difficult to determine a priori. Hence we use it as a free parameter to fit the continuum model to atomistic data at stress $\sigma = 2.07$ GPa, which gives $a = 1.60b$.

The resulting energy barrier $E_{\mathrm{b}}^{\mathrm{I}}$ as a function of stress is plotted as the dashed line in Figure 1b. Clearly, as the stress goes above the fitted value (2.07 GPa), there exists a significant discrepancy between the continuum model prediction and the atomistic data. In particular, the atomistic data predicts that the energy barrier vanishes at 2.83 GPa, while model I predicts the energy barrier vanishes at a higher stress value. The predicted energy barrier also depends on the choice of core radius a. Estimates of a from atomistic simulations are usually less than b [15, p. 232]. For example, if we take $a = 0.63b$, the energy barrier becomes significantly higher and does not vanish even at 3.6 GPa, as shown in Figure 1c.

Allowing the dislocation loop to change its shape at constant area (see Supplementary materials) leads to a slight decrease of $E(A;\sigma)$ (by a few percent) and no significant change in the final prediction of $E_{\mathrm{b}}^{\mathrm{I}}(\sigma)$, especially if the core radius is treated as a fitting parameter. Hence for simplicity this possibility is excluded from subsequent discussions.

Model II now allows the magnitude of the Burgers vector to be a variable b_f that goes from 0 to b, and the energy of the dislocation loop becomes

$$E(b_f,A;\sigma) = 2\pi R\,\frac{\mu b_f^2}{8\pi}\left[\frac{2-\nu}{1-\nu}\left(\ln\frac{8R}{a}-2\right)+\frac{1}{2}\right] + \left[\gamma_{\mathrm{GSF}}(b_f+u_0)-\gamma_{\mathrm{GSF}}(u_0)\right]A - b_f\sigma A \tag{2}$$

where the first term (elastic energy) is now proportional to b_f^2 and the second term involves a non-linear function $\gamma_{\mathrm{GSF}}(u)$, which is called the generalized stacking fault energy (GSF). The GSF curve is computed (see Supplementary materials) from the EAM potential by cutting a perfect crystal into two halves across the (1 1 1) slip plane and sliding them relative to each other along the $[1\,1\,\bar{2}]$ direction by distance u, as shown in Figure 2a. The result is shown as filled circles in Figure 2c.

u_0 Represents the spontaneous slip between the two halves of the crystal in state $\mathcal{A}$ (i.e. before dislocation nucleation) when a shear stress is applied. The nucleation of a dislocation loop will further increase the slip inside the dislocation loop to $u = b_f + u_0$.[1] For each applied stress σ, u_0 is solved numerically from the condition $\partial\gamma_{\mathrm{GSF}}(u)/\partial u|_{u=u_0} = \sigma$.

The energy barrier $E_{\mathrm{b}}^{\mathrm{II}}(\sigma)$ is obtained by finding the saddle point in the two-dimensional landscape of Eq. (2) at the specified stress. The results are plotted as triangles in Figure 1b and c. In Figure 1b, the core radius is fitted to the atomistic data at $\sigma = 2.07$ GPa, which gives $a = 0.99b$. Figure 1c plots the prediction based on $a = 0.63b$. For both choices of a, model II predicts that the dislocation nucleation barrier vanishes close to $\sigma_c = 3.24$ GPa, which is the ideal shear strength defined as $\sigma_c \equiv \max(\partial\gamma_{\mathrm{GSF}}(u)/\partial u)$. When $\sigma = \sigma_c$, the two halves of the crystal separated by the slip plane can shear relative to each other without experiencing any energy

[1] Our expression $u = b_f + u_0$ corresponds to Rice's expression $\Delta = \delta + h\tau/\mu$ in Ref. [19]. The distinction between u and b_f is sometimes ignored in the literature [10]. We find that this would significantly increase in the predicted energy barrier.

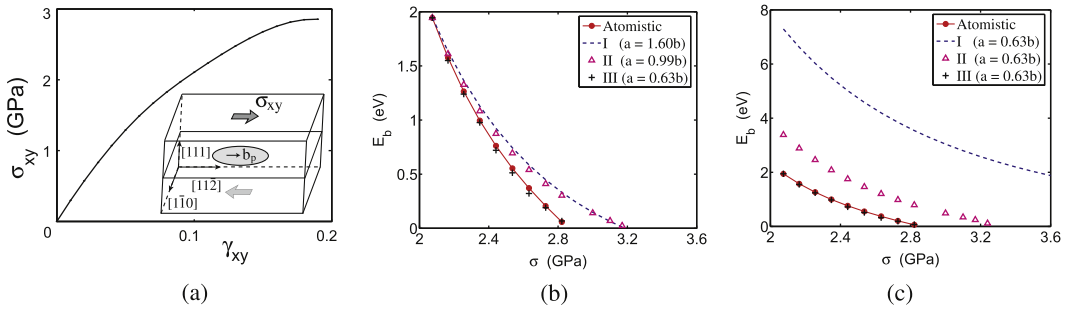

Fig. 1. (a) Shear stress–strain curve of the Cu perfect crystal. The inset shows a schematic of the simulation cell. b_p represents the Burgers vector of the partial dislocation loop. (b) Energy barrier of a homogeneous dislocation loop nucleation as a function of applied shear stress. Predictions from the atomistic are compared with those from continuum models I–III, each using a different core radius a. (c) Same as (b) except that $a = 0.63b$ is used for all continuum models.

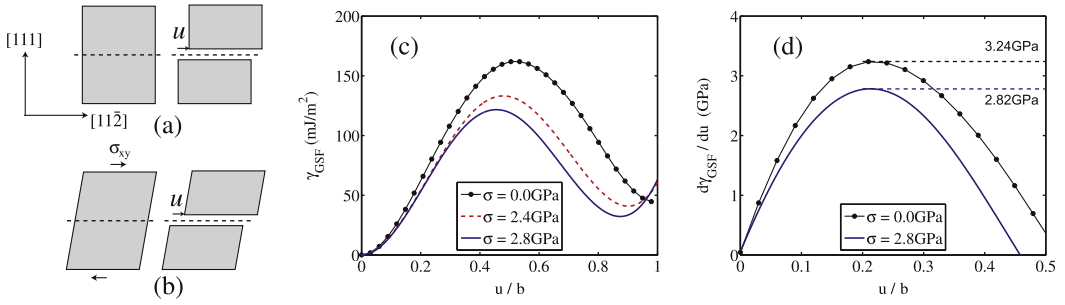

Fig. 2. Schematic for computing the GSF energy (see text). (a) Two half crystals subjected to zero stress rigidly slide against each other to give $\gamma_{\mathrm{GSF}}(u)$. (b) Two half crystals subjected to pure shear stress rigidly slide against each other to give $\gamma_{\mathrm{GSF}}(u;\sigma_{xy})$. (c) GSF energy at zero stress (black solid line) and non-zero shear stresses. (d) Derivative of the GSF curves, whose maxima give measures of the ideal shear strength.

barrier. For self-consistency the dislocation nucleation barrier must be zero at σ_c, which is satisfied by model II.[2]

However, there still exists a discrepancy between model II and the atomistic data. The atomistic data shows that homogeneous dislocation nucleation becomes barrierless at 2.83 GPa, which is lower than the ideal shear strength σ_c (3.24 GPa) defined above. This means that the crystal collapses well before σ_c, hence the definition of the ideal shear strength has to be modified.

While it is customary to compute the GSF curve by rigidly sliding two blocks of perfect crystals at zero strain, the discrepancy noted above suggests the need to consider the effect of shear strain on the crystal on the GSF curve. We perform the following calculations to investigate this effect. For each given stress value σ, the strain of the perfect crystal is first adjusted so that $\sigma_{xy} = \sigma$ is the only non-zero stress value. The strained crystal is then cut into two halves along the (1 1 1) plane and the two halves are displaced relative to each other along the $[1\,1\,\bar{2}]$ direction (allowing vertical relaxation), as shown in Figure 2b. This gives rise to a family of GSF curves, $\gamma_{\mathrm{GSF}}(b_f;\sigma)$, each for a different stress value σ, as shown in Figure 2c. Using $\gamma_{\mathrm{GSF}}(b_f;\sigma)$ as the input, the dislocation energy in model III is

$$E(b_f, A;\sigma) = 2\pi R\,\frac{\mu b_f^2}{8\pi}\left[\frac{2-\nu}{1-\nu}\left(\ln\frac{8R}{a}-2\right)+\frac{1}{2}\right] + \left[\gamma_{\mathrm{GSF}}(b_f+u_0;\sigma)-\gamma_{\mathrm{GSF}}(u_0;\sigma)\right]A - b_f\,\sigma\,A \tag{3}$$

From Eq. (3), the energy barrier $E_{\mathrm{b}}^{\mathrm{III}}(\sigma)$ is obtained using the same approach as in model II, and the results are shown in Figure 1b, with $a = 0.63b$. Finally, excellent agreement between model III and atomistic data is observed. In particular, model III predicts that dislocation nucleation energy barrier vanishes at $\sigma = 2.83$ GPa, in agreement with the atomistic calculations.

The above analysis reveals that the "true" ideal shear strength for this EAM model of Cu is $\widehat{\sigma}_c = 2.8$ GPa, instead of $\sigma_c = 3.2$ GPa. Recall that σ_c is defined as $\sigma_c \equiv \max_{b_f} \partial/\partial_{b_f}\gamma_{\mathrm{GSF}}(b_f;0)$ in which the use of the GSF curve at zero stress indicates an inconsistency. On the other hand, $\widehat{\sigma}_c$ is defined as the lowest root of the implicit equation: $\widehat{\sigma}_c = \max_{b_f} \partial/\partial_{b_f}\gamma_{\mathrm{GSF}}(b_f;\widehat{\sigma}_c)$ Although the definition of $\widehat{\sigma}_c$ is more complex, it can be easily solved numerically, as is done here.

There have been multiple definitions of ideal shear strengths in the literature. An alternative definition to the resistance to rigid body sliding is the maximum stress $\sigma_{\max}$ in the crystal subjected to uniform (affine)

[2] This condition is not satisfied by model I for $a = 0.63b$, because model I does not contain GSF as its input.

deformation [20]. The $\widehat{\sigma}_c$ defined above is lower than both σ_c and $\sigma_{\max}$ for the EAM model of Cu considered here (see Supplementary materials), and is hence a more physical measure of the ideal shear strength. It shows that the crystal fails by localized shear between two adjacent atomic planes, while the resistance against this instability is reduced by the uniformly distributed shear strain in the crystal.

The concept of a family of GSF curves, one for each stress value, is related to the multi-layer GSF proposed by Ogata et al. [21] to study the nucleation of twinning. Here, every pair of neighboring layers slide against each other due to the uniform shear strain set up by the applied stress. Figure 2d shows that shear stresses in the GPa range have a strong effect on the GSF curves and is responsible for reducing the ideal shear strength from 3.2 to 2.8 GPa. While the effect of normal stress perpendicular to the slip plane on the GSF curve has been recognized before [22], here we show that the very shear stress that drives the dislocation nucleation affects the GSF curve significantly.

We have identified the necessary ingredients for a two-variable continuum model to reproduce the energy barrier of homogeneous dislocation nucleation predicted by explicit atomistic calculations. First, the Burgers vector needs to be able to vary continuously during the nucleation process. Second, the applied stress alters the generalized stacking fault energy and a family of GSF curves parameterized by stress need to be used as inputs to the continuum model. One limitation of the present model (model III) is the treatment of core radius a as a fitting parameter. Alternatively, one can compute the core radius (corresponding to zero core energy) from atomistic simulations [23]. Nonetheless, the fitted value $(a = 0.63b)$ is consistent with earlier estimates. The continuum models presented here can be extended to predict the energy barrier for dislocations nucleating near free surfaces, provided the effect of image stress [24,25] is properly accounted for. The models can be further extended to finite temperatures by using the GSF free energy curves [26] as inputs.

We thank Prof. W.D. Nix and Dr. Christopher R. Weinberger for useful discussions. The work was partly supported by National Science Foundation Career Grant CMS-0547681 and the Army High Performance Computing Research Center at Stanford.

Supplementary data associated with this article can be found, in the online version, at doi:10.1016/j.scriptamat.2011.02.023.

[1] C.L. Kelchner, S.J. Plimpton, J.C. Hamilton, Phys. Rev. B 58 (1998) 11085.
[2] Z.W. Shan, R.K. Mishra, S.A.S. Asif, O.L. Warren, A.M. Minor, Nature Mater. 7 (2008) 115.
[3] P. Hänggi, P. Talkner, M. Borkovec, Rev. Mod. Phys. 62 (1990) 251.
[4] T. Zhu, J. Li, A. Samanta, A. Leach, K. Gall, Phys. Rev. Lett. 100 (2008) 025502.
[5] F. Frank, Symposium on Plastic Deformation of Crystalline Solids, Carnegie Institute of Technology, Pittsburgh, PA, 1950, p. 89.
[6] G. Xu, A.S. Argon, Philos. Mag. Lett. 80 (2000) 605.
[7] M. de Koning, W. Cai, V.V. Bulatov, Phys. Rev. Lett. 91 (2003) 025503.
[8] G. Xu, F.R.N. Nabarro, J.P. Hirth, Dislocations in Solids, Elsevier, 2004.
[9] E. Rabkin, H.-S. Nam, D.J. Srolovitz, Acta Mater. 55 (2007) 2085.
[10] M.Y. Gutkin, I.A. Ovid'ko, Acta Mater. 56 (2008) 1642.
[11] Y. Xiang, H. Wei, P. Ming, W. E, Acta Mater. 56 (2008) 1447.
[12] G. Henkelman, B.P. Uberuaga, H. Jónsson, J. Chem. Phys. 113 (2000) 9901.
[13] W. E, W. Ren, E. Vanden-Eijnden, Phys. Rev. B 66 (2002) 052301.
[14] Y. Mishin, M.J. Mehl, D.A. Papaconstantopoulos, A.F. Voter, J.D. Kress, Phys. Rev. B 63 (2001) 224106.
[15] J.P. Hirth, J. Lothe, Theory of Dislocations, Wiley, New York, 1982.
[16] K. Kang, Ph.D. Thesis, Stanford University, 2010.
[17] W. Cai, A. Arsenlis, C.R. Weinberger, V.V. Bulatov, J. Mech. Phys. Solids 54 (2006) 561.
[18] R.O. Scattergood, D.J. Bacon, Philos. Mag. 31 (1975) 179.
[19] J.R. Rice, J. Mech. Phys. Solids 40 (1992) 239.
[20] D. Roundy, M.L. Cohen, Phys. Rev. B 64 (2001) 212103.
[21] S. Ogata, J. Li, S. Yip, Science 298 (2002) 807.
[22] V.V. Bulatov, E. Kaxiras, Phys. Rev. Lett. 78 (1997) 4221.
[23] W. Cai, V.V. Bulatov, J. Chang, J. Li, S. Yip, Philos. Mag. 83 (2003) 539.
[24] C.R. Weinberger, W. Cai, J. Mech. Phys. Solids 55 (2007) 2027.
[25] C.R. Weinberger, S. Aubry, S.-W. Lee, W.D. Nix, W. Cai, Model. Simul. Mater. Sci. Eng. 17 (2009) 075007.
[26] D.H. Warner, W.A. Curtin, Acta Mater. 57 (2009) 4267.